Rare Metal Materials and Engineering
Volume 46, Issue 11, November 2017
Online English edition of the Chinese language journal

Available online at www.sciencedirect.com
ScienceDirect

Cite this article as: Rare Metal Materials and Engineering, 2017, 46(11): 3253-3259.

ARTICLE

Synthesis of Cobaltous Nickel Oxide Core/Shell Nanowires for Supercapacitors

Xing Fangkai[1,2], Ren Haoqi[3], Ji Chenchen[1], Zhang Yuanping[1], Yang Shengchun [1]

[1]MOE Key Laboratory for Non-equilibrium Synthesis and Modulation of Condensed Matter, State Key Laboratory for Mechanical Behavior of Materials, Xi'an Jiaotong University, Xi'an 710049, China; [2] Xi'an University of Technology, Xi'an 710048, China; [3] Fudan University, Shanghai 200433, China

Abstract: CoO/NiO core/shell nanowires (NWs) were synthesized using an efficient two-step approach. The detailed structural analysis through the transmission electron microscopy indicate that the CoO NW core is well enclosed by the NiO nanoflake shell with an unique nanoporous structure. Due to these structural advantages, when the obtained CoO/NiO core/shell NW material is used as a supercapacitor electrode, it presents a much enhanced capacitance (708 F g^{-1} at 1 A g^{-1}), better rate capability and excellent cycling performance (>80 % capacitance retention for 1000 cycles) compared with the single component samples. Besides, the synergetic interaction between the CoO NWs and NiO nanoflakes can produce more active sites for redox progresses than single material during the electrochemical reaction, which can provide synergistic effect to the capacitance and electrochemical stability.

Key words: CoO; NiO; core/shell; nanowires; supercapacitor

In recent years, there is a boom in development of renewable energy production from sun, water and wind, due to the increasingly severe issue of climate change and lessened reserves of fossil fuels. Consequently, batteries and electrochemical capacitors (ECs), the two major energy storage systems, become indispensable and significant in daily lives. ECs, known as supercapacitors, have splendid qualities such as high power density, fast charge/discharge characteristic, and long cycle life[1-3], making them suitable for backup, main power and alternating power sources[4]. Depending on the different charge storage mechanisms, ECs can be classified into pseudocapacitors and electrical double-layer capacitors (EDLCs)[5]. As for the electrode materials, there are three main categories: carbon materials, faradaic materials and conducting polymers[6,7]. However, each kind of these single components has advantages and disadvantages, and to combine the strong points of those materials and thus to achieve better performance, a number of works on different kinds of composites have been published, such as carbon/carbon[8], carbon/metal oxide[9-12], carbon/metal[13], carbon/polymer[14], metal/metal oxide[15-18], metal oxide/metal oxide[19-22], polymer/metal[23], polymer/polymer[24] and carbon/polymer/metal[25], and their enhanced properties have been exhibited.

Among the explored systems, transition metal oxides have been studied extensively due to their surface redox reactivity properties. Such materials possess various oxidation states and exhibit electrochemical faradaic redox reactions between materials and ions in the electrolyte at a appropriate voltage range[26,27], and provide higher energy density than carbon and better cycling performance than conducting polymers[7]. To meet the general requirements in ECs application, transition metal oxides such as manganese oxide, ruthenium oxide, vanadium oxide, nickel oxide and cobalt oxide are considered. In view of high energy density, good cyclic performance, low cost and natural abundance, NiO and CoO have drawn wide attention for ECs devices[28-30]. However, pure NiO materials show poor

Received date: November 17, 2016
Foundation item: National Natural Science Foundation of China (51271135)
Corresponding author: Ji Chenchen, Ph. D., School of Science, MOE Key Laboratory for Non-equilibrium Synthesis and Modulation of Condensed Matter, State Key Laboratory for Mechanical Behavior of Materials, Xi'an Jiaotong University, Xi'an 710049, P. R. China, Tel: 0086-29-82663034, E-mail: jichenchen2013@stu.xjtu.edu.cn

conductivity, which limits their applications[31]. More recently, the influence of composition on the activation energy of conductivity has been revealed, and it is found that the addition of CoO has a strong influence on NiO[32]. Moreover, CoO as a transitional metal oxide could also make a contribution to the pseudocapacitance[33]. Therefore the research on their mixed composition is quite worthwhile, and the hybrid electrode is expected to display an enhanced electrochemical performance.

Herein, we present an efficient two-step method to fabricate the CoO/NiO core/shell NWs which possess porous structure and high performance for ECs. The electrode based on CoO/NiO core/shell NW material presents a higher specific capacitance (708 F g^{-1} at 1 A g^{-1} and 403 F g^{-1} at 10 A g^{-1}) and an excellent cycling performance in KOH electrolyte than that of the single component samples. This enhanced performance benefits from their unique core/shell and porous structure, which could conduce to ion and electron diffusion, reduce the diffusion length for the anions transferred, and produce more active sites for faradic redox reaction during the charge/discharge process. On account of the good properties, the active materials we fabricated have potential in chemical sensing, catalysis, electronics, and industrial electricity devices.

1 Experiment

All the chemicals were of analytical grade and were used directly without further purification. Firstly, the $Co(OH)_2$ NWs sample was prepared by a hydrothermal method. The solution was prepared by dissolving 0.8 mmol of $CoCl_2$, 4 mmol of $CO(NH_2)_2$, and 7.7 mg of PVP in 30 mL of de-ionized (DI) water. Then the obtained solution was transferred into a 50 mL sealed Teflon-lined stainless steel autoclave and maintained at 120 ℃ for 6 h and then cooled to room temperature, the product was obtained by washing with DI water and ethanol for several times. Secondly, the as-prepared $Co(OH)_2$ NWs were used as the backbone for the NiO nanoflake growth by a facile chemical bath deposition (CBD)[34]. The solution for CBD was prepared by mixing 5 mL of 1 mol/L nickel sulfate, 3.75 mL of 0.25 mol/L ammonium persulfate, and 1.25 mL of aqueous ammonia. The as-prepared $Co(OH)_2$ NWs were added in the fresh obtained solution, kept at 25 ℃ for 30 min and then the obtained sample was filtered, washed and dried. Finally, the obtained samples were annealed at 350 ℃ for 1.5 h under Ar gas protection. As a control sample, pure CoO NWs and NiO nanoflakes were prepared using the same process as mentioned above.

The crystallographic structures of the samples were characterized by powder X-ray diffraction (XRD, Bruker D8 Advance X-ray diffractometer) equipped with a Cu Kα X-ray source (λ=0.154 05 nm). The morphology and microstructure of the samples were investigated by scanning electron microscopy (SEM, JEOL JSM-7000F) and transmission electron microscopy (TEM, JEOL JEM-3010). The STEM images were obtained from a FEI Tecnai G2 F30 S-Twin transmission electron microscope at an accelerating voltage of 300 kV.

The electrochemical measurements were tested in a three-electrode system in 2 mol/L KOH aqueous electrolyte. A platinum plate (1 cm^2) was used as the counter electrode and a saturated calomel electrode (SCE) was used as the reference electrode. The obtained samples were used as the working electrode, which were prepared by mixing 85wt% of the obtained samples, 5wt% of acetylene black (AB) and 10wt% of polytetrafluoroethylene (PTFE), and then the mixture was pressed onto a nickel grid (1 cm^2). The typical loading of the electroactive material is about 5 mg cm^{-2}. Cyclic voltammetry (CV) and galvanostatic charge/discharge (GCD) tests were performed on a electrochemical workstation (Chenhua CHI660e, Shanghai). The galvanostatic charge/discharge cycling performance was tested on a LAND battery test system. The specific capacitance was calculated from the GCD curves according to the following equation:

$$C_{sc}=(I\Delta t)/(m\Delta V) \quad (1)$$

Where, C_{sc} (F/g) is the specific capacitance, I (A), Δt (s), m (g), and ΔV(V) represent the discharge current, total discharge time, mass of active materials, and discharging potential windows, respectively.

2 Results and Discussion

In this work, a two-step solution method was used to fabricate the CoO/NiO core/shell NWs. A hydrothermal method was firstly employed to synthesize the $Co(OH)_2$ NWs, and the obtained $Co(OH)_2$ NWs was then severed as the core scaffold for the deposition of $Ni(OH)_2$ nanoflakes branch shell in the second step. After the heating treatment, CoO/NiO core/shell nanowires were obtained. Fig.1 shows the XRD patterns of the CoO/NiO core/shell NWs, CoO NWs and NiO nanoflake samples. The diffraction peaks at 36.4°, 42.4°, 61.4°, 73.6°, 77.6° and 37.3°, 43.3°, 62.7°, 75.4°can be assigned to the cubic CoO and NiO structure, respectively.

The morphologies of the obtained $Co(OH)_2$ precursor, CoO and the CoO/NiO core/shell NWs samples are shown in Fig.2. The $Co(OH)_2$ precursor displays a nanowire structure with smooth surface, and the average diameter of the nanowire is about 90 nm (Fig.2a). After the heating treatment to the $Co(OH)_2$ precursor, the obtained CoO NWs become porous (Fig.2b). As for the obtained CoO/NiO core/shell nanowire sample, Fig.2c and Fig.2d show that the CoO NWs are tightly covered by the NiO nanoflakes. And the shell thickness does not increase because of the NiO layers form a passivating layer that prevents their

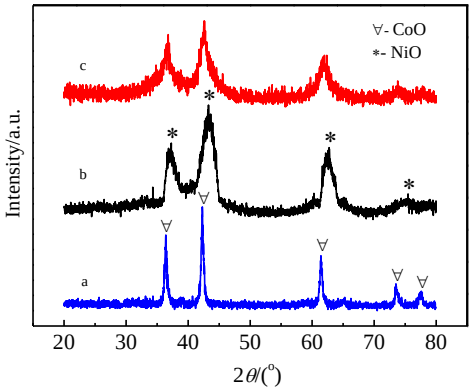

Fig.1 XRD patterns of the CoO/NiO core/shell NWs (a), NiO nanoflake (b), and CoO NW samples (c)

further growth[16]. In addition, the NiO nanoflakes are interconnected to construct a porous structure, presenting a unique porous core/shell heterostructure.

TEM images of the $Co(OH)_2$ precursor and CoO samples are shown in Fig.3a and Fig.3b, which show that the two samples both display a nanowire structure. After the heating treatment, the $Co(OH)_2$ precursor is transformed into a porous structure, which are consistent with the SEM results. Fig.3c demonstrates the porous core/shell heterostructure of an individual nanowire in detail. It can be easily observed that the CoO NW core and the NiO nanoflake shell from the TEM images, and the CoO NWs core are tightly covered by the porous NiO nanoflakes shell. Fig.3d~3h show the STEM EDS elemental mapping results of the CoO/NiO core/shell NWs sample. The EDS scanning images further prove the core/shell NW heterostructure of the prepared sample, where element Co is only found in the core and elements Ni are homogeneously distributed throughout these nanoflakes shell.

The porosity of the CoO/NiO core/shell NWs sample was characterized by the N_2 adsorption/desorption measurement (Fig.4). A type IV hysteresis can be observed at a relative pressure of 0.45~1.0 in the N_2 adsorption/desorption isotherms, which indicates that the prepared sample exhibits a mesoporous characteristic. The BET surface area of the CoO/NiO core/shell NWs sample is about 81.7 $m^2 \cdot g^{-1}$, and mainly consists of mesopores centered at 20 nm (Fig.4, inset).

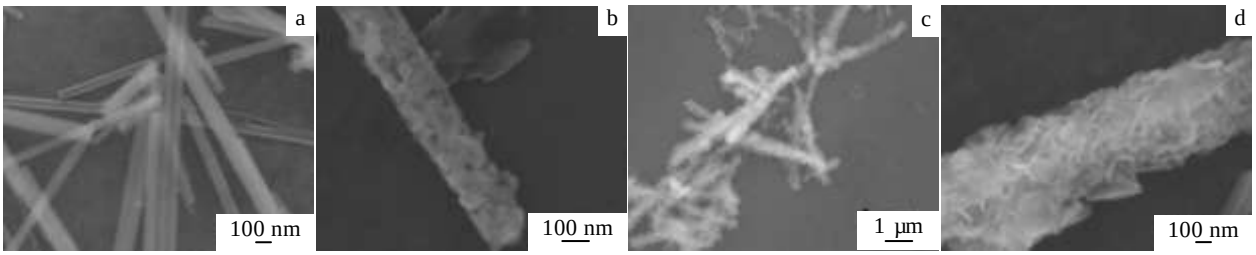

Fig.2 SEM images of the $Co(OH)_2$ NWs (a), CoO NWs (b) and CoO/NiO core/shell NWs (c, d)

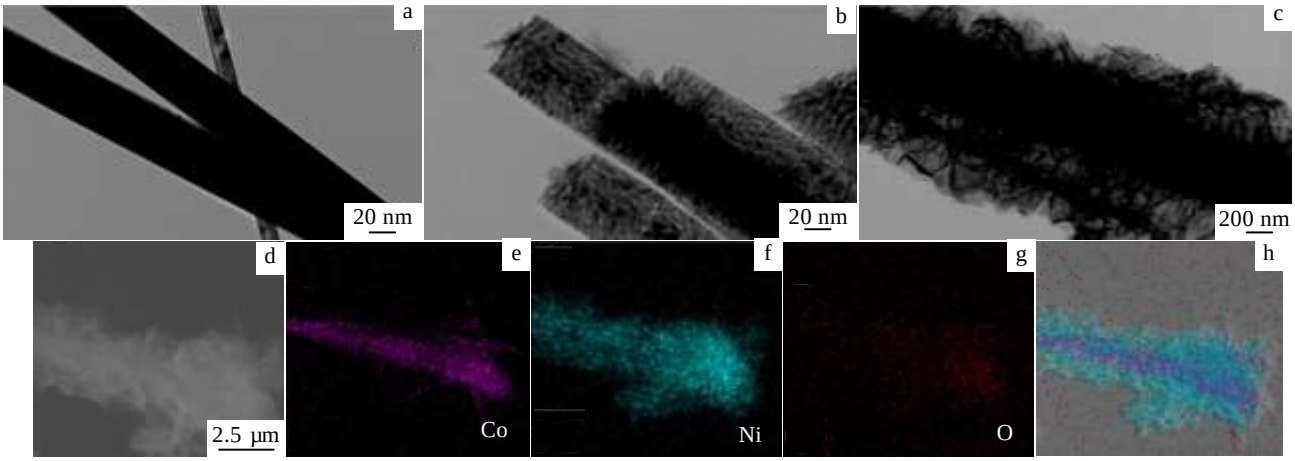

Fig.3 TEM images of the $Co(OH)_2$NWs (a), CoO NWs (b), CoO/NiO core/shell NWs (c); (d) STEM image and (e~h) EDS elemental mappings of the CoO/NiO core/shell NWs with different color for different elements

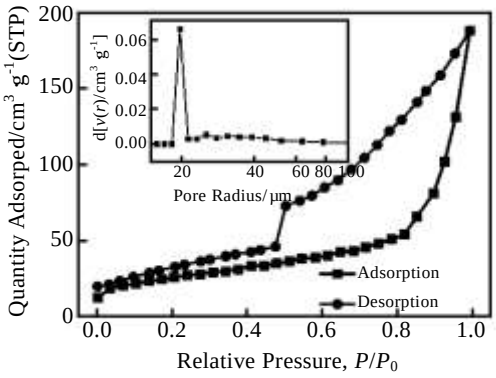

Fig.4 Nitrogen adsorption/desorption isotherm of the CoO/NiO core/shell NWs sample (the inset shows the BJH pore-size distribution)

The possible formation mechanism of the core/shell structure is likely involved the "oriented attachment" and "self-assembly" processes. At the first stage, Ni-based hydroxide mesocrystals could form due to the precipitin reaction between the Ni^{2+} cation and OH^- anion in the reaction system. Then the formed adjacent Ni-based hydroxide mesocrystals would spontaneously self-assembled together by sharing a common crystallographic orientation and deposit prior onto the surface of $Co(OH)_2$ NWs cores. And the $Co(OH)_2$ NWs can be regarded as active nucleation centers. These active sites would reduce the overall interfacial energy barrier for the following growth of Ni-based hydroxide shell[19,20]. In the next stage, these particles would join at a planar interface and bond together to minimize the overall surface energy of the particles[22,35,36]. As the reaction proceeds, the growth of Ni-based hydroxide mesocrytals led to the formation of the nanoflakes, which were then self-assembled together and covered on the $Co(OH)_2$ core. Finally, a core/shell NWs structure was formed.

The electrochemical performance of the CoO/NiO core/shell NWs for their potential application in supercapacitor were tested by CV and GCD measurements. The CoO/NiO core/shell NWs electrodes were measured in a three-electrode system, containing 2 mol/L KOH aqueous solution as the electrolyte. Fig.5a depicts the typical CV curves of the CoO/NiO core/shell NWs electrodes at different scan rates. A pair of strong redox peaks are clearly observed within the electrochemical window of 0.0~0.45 V (vs. SCE) in each curve, indicating that Faradaic redox reactions on the electrode surface occur, which are obviously distinct from the typical rectangular CV shape of the EDLCs[15]. Notably, the redox peak potentials vary slightly with the increase of the scan rate, suggesting low polarization of the CoO/NiO core/shell NWs electrode.

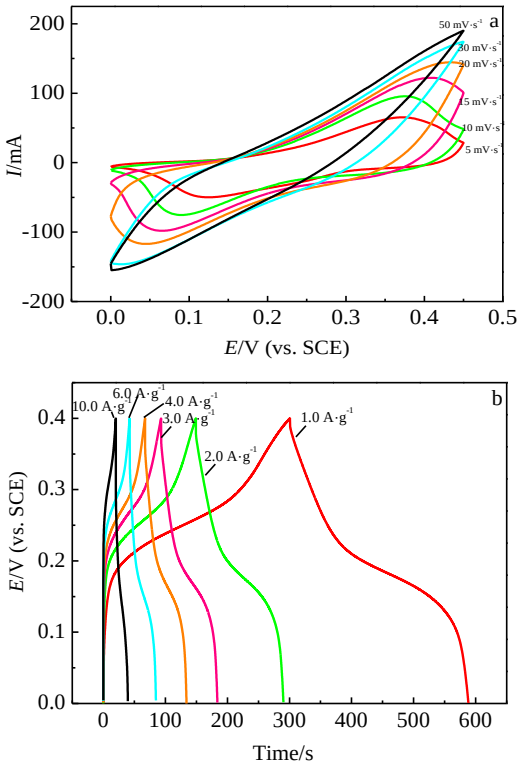

Fig.5 CV curves at various scan rates (a) and GCD curves of the CoO/NiO core/shell NWs (b)

The discharge plateau in the GCD curves for the CoO/NiO core/shell NWs electrode can be observed at different current densities (Fig.5b), which indicates a favorable electrochemical performance and a common pseudocapacitive behavior of the prepared electrode[37]. And this results match well with the CV analysis discussed above.

The comparison of CV results for the CoO/NiO core/shell NWs, NiO nanoflakes and CoO NWs electrodes at a scan rate of 5 mV s^{-1} is presented in Fig.6a. The area for the CV curve can be used to estimate the specific capacitance of the material[38]. It can be seen that the area included in the CV curve for the CoO/NiO core/shell NWs electrode is much larger than that of the NiO nanoflakes and CoO NWs electrodes (Fig.6a), which indicate that the CoO/NiO core/shell NWs have the most excellence capacitive performance among these three electrodes. As for the prepared CoO/NiO core/shell NWs electrode, two possible electrochemical reaction may involve for its charge storage process[12,29,39-42]:

For the NiO component:

$NiO+OH^-\rightarrow NiOOH+e^-$ or $NiO+H_2O\rightarrow NiOOH+H^++e^-$ (2)

For the CoO component:

$CoO+OH^- \rightarrow CoOOH+e^-$

and $CoOOH+OH^- \rightarrow CoO_2+H_2O+e^-$ (3)

Besides, the CoO/NiO core/shell NWs possess the highest peak currents among three samples, which indicate that the electrochemical reaction activity of the CoO/NiO core/shell NWs is higher than those of the single components samples.

Furthermore, the specific capacitances were calculated based on the GCD plots. The specific capacitance values were calculated to be 708, 672, 637, 620, 558, 403 F g^{-1} at current densities of 1, 2, 3, 4, 6 and 10 A g^{-1}, respectively, much higher than that of the single component samples prepared in our work (Fig.6b). The specific capacitance values of the obtained CoO/NiO core/shell NW electrode are also higher than that of the other monometallic oxides of CoO or NiO reported in the literature such as snowflake-like CoO (97 F/g at 0.625 A/g)[43], nest-like CoO nanofibers (670.7 F/g at 0.2 A/g)[44], flower-like NiO microspheres (324 F/g at 2 A/g)[45], porous NiO (532 F/g at 2 A/g)[46], porous NiO nanocrystal (686 F/g at 1 A/g)[47]. Besides, the specific capacitance values of the prepared electrode are also higher than that of the binary metal oxide such as mesoporous CoO-doped NiO hexagonal nanoplatelets (170 F/g at 1 mA/cm^2)[48], wire-like NiO/Co_3O_4 composite (184 F/g at 1 A/g)[49], $Co_3O_4/NiCo_2O_4$ core/shell arrays (672 F/g at 0.5 A/g)[50]. The CoO/NiO core/shell NWs also show the best rate capability among the three samples. When the current density increases from 1 to 6 A g^{-1}, 79% of capacitance is retained, which is higher than those for the CoO NWs (74%) and NiO nanoflakes (76%), as depicted in Fig.6b. It can be reckoned that the specific capacitance increases remarkably as the current density decreases for all the three samples. And this can be ascribed to the limited OH^- ions diffusion which cannot meet well the need of fast electrochemical reaction at high current densities[40,41].

Moreover, a repeated charging/discharging measurement was used to evaluate the cycling stability of the CoO/NiO core/shell NW electrode. As shown in Fig.7, the specific capacitance of the CoO/NiO core/shell NW electrodes increases from 600 to 900 F g^{-1} at the initial cycling process, most likely due to the electrolyte penetrate into the bulk of the CoO/NiO core/shell NW samples. However, the single component sample possesses lower specific capacitance (400 F g^{-1} for the NiO nanoflakes and 150 F g^{-1} for the CoO NWs). Besides, the core/shell NW electrodes keep 80 % of the initial capacitance value after 1000 cycles at 2 A g^{-1}, exhibiting a good cycling stability of the prepared CoO/NiO core/shell NW.

Based on the above results, the CoO/NiO core/shell NWs sample was manifested to possess a better electrochemical performance than the single component samples. Its enhanced performance benefits from the CoO NW core, the NiO nanoflake shell, and the unique porous nano-structure.

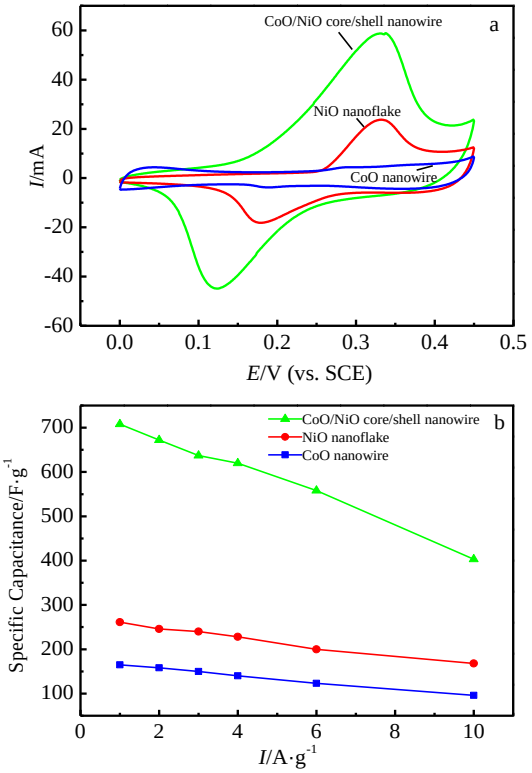

Fig.6 CV curves of the three electrodes at a scan rate of 5 mV s^{-1} after 10th cycle (a); specific capacitances at different current densities for the three electrodes (b)

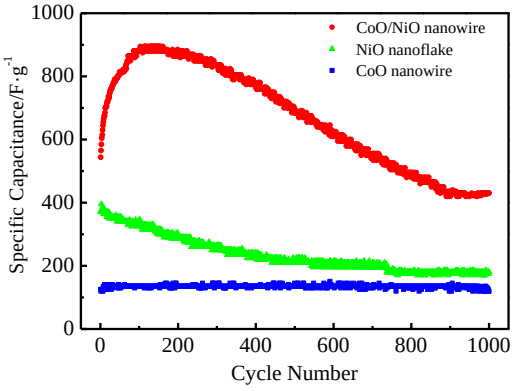

Fig.7 Cycling performance of the CoO NWs, NiO nanoflakes and the CoO/NiO core/shell NWs at 2 A g^{-1}

Firstly, the CoO nanowire cores are closely covered with the NiO porous shells, which would enable the full exposure of both the core and the shell to the electrolyte, conduce to ion and electron transport and reduce the diffusion length for OH^- transfer during the charge/discharge process[3]. And therefore, the space between the core and the shell is abundantly used due to the porous structure.[20] Secondly, the synergetic interaction

between the CoO NWs and NiO nanoflakes produces more active sites for redox progresses than single material during the electrochemical reaction. Both CoO and NiO are active for electro-redox progress, which could work together and provide synergistic effect for a higher electrochemical ability[21]. Lastly, the core/shell configuration has a firm mechanical and phase stability. The porous structure can also accommodate the volume change during cycling and alleviate the structure or phase damage caused by the redox reaction, which would improve the stability of the capacitor[15,24].

3 Conclusions

1) A facile and efficient method is proposed for the synthesis of CoO/NiO core/shell NW sample. The obtained sample displays a hierarchical structure, which is constructed by the CoO NW core coated with NiO porous shell. When the obtained sample fabricated as the active material used for ECs, the CoO/NiO core/shell NW sample exhibits the highest specific capacitance, best rate performance and cycling stability compared with the single component sample of NiO nanoflakes and CoO NWs. A specific capacitance of 708 $F{\cdot}g^{-1}$ at 1 $A{\cdot}g^{-1}$ is obtained for the CoO/NiO core/shell NWs. Meanwhile the capacitance maintains ~80 % after 1000 cycles without relaxation.

2) This work not only offers the possibilities for designing efficient electrode materials for supercapacitors, but also provides advanced insights into improving their electrochemical performance by means of structural modification.

References

1 Simon P, Gogotsi Y. *Nature Materials*[J], 2008, 7(11): 845
2 Winter M, Brodd R J. *Chemical Reviews*[J], 2004, 104: 4245
3 Yuan C, Zhang L, Hou L *et al. RSC Advances*[J], 2014, 4(28): 14 408
4 Conway B E. *Electrochemical Supercapacitors: Scientific Fundamentals and Technological Applications*[M]. New York: Kluwer Academic/Plenum Publishers, 1999
5 Kötz R, Carlen M. *Electrochimica Acta*[J], 2000, 45: 2483
6 Sarangapani S, Tilak B V, Chen C P. *Journal of the Electrochemical Society*[J], 1996, 143: 3791
7 Wang G, Zhang L, Zhang J. *Chemical Society Reviews*[J], 2012, 41: 797
8 Maiti S, Das A K, Karan S K *et al. Journal of Applied Polymer Science*[J], 2015, 132: 42 118
9 Jin Y, Chen H, Chen M *et al. ACS Applied Materials and Interfaces*[J], 2013, 5: 3408
10 Gao H, Xiao F, Ching C B *et al. ACS Applied Materials and Interfaces*[J], 2012, 4(12): 7020
11 Xiao X, Li, T, Yang P *et al. Acs Nano*[J], 2012, 6(10): 9200
12 Wang C, Xu J, Yuen M F *et al. Advanced Functional Materials*[J], 2014, 24: 6372
13 Ye S, Feng J, Wu P. *ACS Applied Materials and Interfaces*[J], 2013, 5(15): 7122
14 Jeon I Y, Tan L S, Baek J B. *Journal of Polymer Science Part A: Polymer Chemistry*[J], 2010, 48(9): 1962
15 Wu L C, Chen Y J, Mao M L *et al. ACS Applied Materials Interfaces*[J], 2014, 6: 5168
16 Johnston-Peck A C, Wang J, Tracy J B. *ACS Nano*[J], 2009, *3*: 1077
17 Han J, Lin Y C, Chen L *et al. Advanced Science*[J], 2015, 2: 1500 067
18 Xia X H, Tu J P, Zhang Y Q *et al. RSC Advances*[J], 2012, 2: 1835
19 Xia X, Tu J, Zhang Y *et al. ACS Nano*[J], 2012, 6(6): 5531
20 Guan C, Liu J, Cheng C *et al. Energy & Environmental Science*[J], 2011, 4: 4496
21 Wu J B, Li Z G, Huang X H *et al. Journal of Power Sources*[J], 2013, 224: 1
22 Mai L Q, Yang F, Zhao Y L *et al. Nature Communications*[J], 2011, 2: 1
23 Chikouche I, Sahari A, Zouaoui A *et al. The Canadian Journal of Chemical Engineering*[J], 2015, 93: 1076
24 Chen C, Fan W, Zhang Q *et al. Journal of Applied Polymer Science*[J], 2015, 132: 42 290
25 Shi K, Pang X, Zhitomirsky I. *Journal of Applied Polymer Science*[J], 2015, 132: 42 376
26 Zhao D D, Bao S J, Zhou W J *et al. Electrochemical Communications*[J], 2007, 9: 869
27 Petitto S C, Marsh E M, Carson G A *et al. Journal of Molecular Catalysis A: Chemical*[J], 2008, 281: 49
28 Zhang Y Q, Xia X H, Tu J P *et al. Journal of Power Sources*[J], 2012, 199: 413
29 Yuan Y F, Xia X H, Wu J B *et al. Electrochimica Acta*[J], 2011, 56: 1208
30 Barreca D, Massignan C, Daolio S *et al. Chemistry of Materials*[J], 2001, 13: 588
31 Parravano G. *The Journal of Chemical Physics*[J], 1955, 23: 5
32 Rao K V, Smakula A. *Journal of Applied Physics*[J], 1965, 36: 2031
33 Yang Z C, Tang C H, Zhang Y *et al. Scientific Reports*[J], 2013, 3: 2925
34 Yan X, Tong X, Wang J *et al. Materials Letters*[J], 2013, 95: 1
35 Niederberger M, Cölfen H. *Physical Chemistry Chemical Physic*[J], 2006, 8: 3271
36 Cölfen H, Antonietti M. *Angewandte Chemie International Edition*[J], 2005, 44: 5576
37 Tang Z, Tang C H, Gong H. *Advanced Functional Materials*[J], 2012, 22: 1272
38 Fan J, Mi H, Xu Y *et al. Materials Research Bulletin*[J], 2013, 48: 1342
39 Xia X H, Tu J P, Zhang J *et al. Solar Energy Materials & Solar Cells*[J], 2008, 92: 628
40 Shahid M, Liu J, Shakir I *et al. Electrochimica Acta*[J], 2012,

85: 243
41 Zhang H, Chen Y, Wang W *et al. Journal of Materials Chemistry A*[J], 2013, 1: 8593
42 Cao L, Xu F, Liang Y Y *et al. Advanced Materials*[J], 2004, 16: 1853
43 Wu C H, Zhu J H, Chen N *et al. Ionics*[J], 2015, 21: 2303
44 Pramanik A, Maiti S, Sreemany M *et al. Journal of Nanoparticle Research*[J], 2016, 18: 93
45 Wu Q, Liu Y, Hu Z. *Journal of Solid State Electrochemistry*[J], 2013, 17: 1711
46 Zeng Y, Wang L, Wang Z *et al. Materials Today Communications*[J], 2015, 5: 70
47 Zhang X, Shi W, Zhu J *et al. Nano Research*[J], 2010, 3: 643
48 Zheng Z, Huang L, Zhou Y *et al. Solid State Sciences*[J], 2009, 11: 1439
49 Liu T, Li Y, Quan G *et al. Materials Letters*[J], 2015, 139: 208
50 Gao X, Zhang Y, Huang M *et al. Ceramics International*[J], 2014, 40: 15 641

氧化钴/镍核壳结构纳米线的合成及其在超级电容器的应用

邢方恺[1,2]，任昊琦[3]，季辰辰[1]，张远平[1]，杨生春[1]

(1. 西安交通大学，陕西省先进功能材料及介观物理重点实验室 物质非平衡合成与调控重点实验室，陕西 西安 710049)

(2. 西安理工大学，陕西 西安 710048)

(3. 复旦大学，上海 200433)

摘　要：通过两步法合成了具有核壳结构的 CoO/NiO 纳米线。TEM 结果显示，CoO 纳米线被 NiO 纳米片层结构紧密包覆，同时该样品具有独特的多孔结构。由于其特殊结构，该样品用于超级电容器电极材料显示了优异的电容性能(当电流密度为 1 A g^{-1} 时，其比容量能够达到 708 F g^{-1})，同时该样品显示了良好的倍率特性以及循环稳定性(当循环 1000 个周期后，其电容保持率为 80%)，其电容性能明显优于单组分样品。这主要是由于 CoO 纳米线和 NiO 纳米片相比于单一组份能够为氧化还原反应提供更多的活性位点，这种协同作用有助于提高材料整体的比容量以及电化学稳定性。

关键词：氧化钴; 氧化镍; 核壳; 纳米线; 超级电容器

作者简介：邢方恺，男，1990 年生，硕士，西安理工大学材料科学与工程学院，陕西省溶（浸）渗重点实验室，陕西 西安 710048，电话：029-82312181，E-mail: xfk@foxmail.com